Extreme Mechanics Letters 48 (2021) 101442

Contents lists available at ScienceDirect

Extreme Mechanics Letters

journal homepage: www.elsevier.com/locate/eml

Dissipative dual-phase mechanical metamaterial composites via architectural design

Weihua Guo [a], Yao Huang [a], Robert O. Ritchie [b,*], Sha Yin [a,*]

[a] Vehicle Energy & Safety Laboratory (VESL), Department of Automotive Engineering, School of Transportation Science & Engineering, Beihang University, Beijing 100191, China
[b] Department of Materials Science & Engineering, University of California, Berkeley, CA 94720, USA

ARTICLE INFO

Article history:
Received 29 May 2021
Received in revised form 9 July 2021
Accepted 11 July 2021
Available online 19 July 2021

Keywords:
Mechanical metamaterials
Lattice materials
Bioinspired design
Architecture
Energy absorption

ABSTRACT

Dual-phase mechanical metamaterials, fabricated as a hybrid of two architected lattice materials with different mechanical properties and bioinspired patterning, have been shown to exhibit improved combination of properties, such as enhanced reinforced strength and toughness. In this study, we specifically examine the selection of the reinforcement phase, specifically involving the effects of its structural architecture, in terms of connectivity and interfacial structure, on the resulting mechanical properties and deformation mechanisms of such dual-phase lattice composites. The composites are simply fabricated using selected laser melting based additive manufacturing. Using quasi-static compression tests and simulation studies, we find that enhancing the role of the reinforcement phase (RP), connection phase (CP) and their interfaces, by employing more trusses distributed along the loading direction, can dramatically improve mechanical properties and energy absorption. By such architectural design of the connection phase, the specific stiffness, specific strength, and specific energy absorption of the dual-phase lattice composites can be optimized, respectively by 77%, 7% and 51% compared to the unreinforced matrix phase lattices. This suggests that the design space of mechanical metamaterials can be significantly expanded by architectural and phase selection together with bioinspired phase patterning.

1. Introduction

Mechanical metamaterials have been widely studied during the past decade; they represent engineering materials with mechanical properties that can be manipulated through changing the architecture and assembly of multiple structural elements, sometimes fashioned from different materials. With the fast development of 3D printing, metamaterials with complex architectures engineered over varying length-scales have been designed and fabricated. For example, ceramic metamaterials consisting of nanoscale hollow tubes have been developed that are simultaneously ultralight, strong, and energy-absorbing; moreover, they can recover their original shape after compression strains in excess of 50% [1]. Novel unit designs have also been reported such as the elastically-isotropic metamaterials developed by Tancogne-Dejean et al. [2] which combine differing truss lattices, including simple cubic (*sc*), body-centered cubic (*bcc*) and face-centered cubic (*fcc*) lattices. In similar vein, Berger et al. [3] identified the "plate lattice", which could achieve the Hashin–Shtrikman upper bounds on isotropic elastic stiffness. Novel metamaterials with outstanding energy absorption have been designed, such as "Shellular", which displays a continuous shell structure [4,5]. Additionally, Bonatti et al. [6] designed a series of octet truss lattice structures including those with solid trusses, hollow trusses and a spherical shell lattice; under quasi-static compression, these shell-based lattices were found to exhibit twice the strength and energy absorption of conventional octet truss lattices.

Additive manufacturing provides the enabling key to processing these metamaterials, as demonstrated by Lei et al. [7] who was able to investigate the effects of hybrid spatial arrangement patterns and cell performance differences on the overall mechanical performances of lattice structures. In addition, through unique structural design, reusable mechanical materials, materials exhibiting negative stiffness and those with controlled thermal expansion have been all fabricated as lattice metamaterials [8].

By comparison, biological materials are generally hybrid composites typically consisting of a hard mineral phase within a soft phase of organic molecules, which are architectured to display often exceptional structural capabilities [9]. As such, numerous design motifs have been utilized in biological materials [10], including the Bouligand architecture coupled with voids to toughen the dactyl club of the mantis shrimp [11], the "brick-and-mortar" architectures in conch shells and nacre [12], and

* Corresponding authors.
E-mail addresses: ritchie@berkeley.edu (R.O. Ritchie), shayin@buaa.edu.cn (S. Yin).

https://doi.org/10.1016/j.eml.2021.101442
2352-4316/

the local reinforcement in pomelo peel to promote excellent energy absorption. Employing a bioinspired philosophy into the design of engineering materials can provide one way to enhance mechanical properties under extreme environmental conditions. Bioinspired composite systems with co-continuous phases have been shown to exhibit excellent stiffness, strength, and energy dissipation [13–15]. Also, bioinspired dual-phase lattice (DPL) composites have been proposed, which are novel mechanical metamaterials that employ an architectured lattice material as their constituent matrix phase (MP) coupled with a reinforcement phase (RP); these dual-phase lattices appear to display excellent mechanical properties with strength, toughness and energy absorption capabilities [16]. However, from the perspective of composite materials, the role of interfaces is invariably critical for their mechanical properties, as has been demonstrated by the various approaches used for carbon fiber composites that employ coatings and surface modification of the fibers to enhance their interfacial properties [17,18]. Additionally, as pointed out by Liu et al., the effective Young's modulus of composites may even surpass the upper Voigt estimate due to the Poisson's ratio effect [19]. Nevertheless, optimizing the architecture of the matrix (MP) and reinforcement phase (RP) and in particular the interphase structure of their connections has remained largely unexplored for dual-phase lattice (DPL) composites.

To provide a design rational for structural DPLs, this study is focused on experimental and simulation studies to aid the selection of such architectures for the MP, RP and connection phase (CP) structures to achieve exceptional mechanical properties. Our approach is to utilize *bcc*, *fcc*-type and *fcc*-based hybrids for each of these RP and CP structures and the phase boundaries to generate DPLs with various truss topologies. Specific lattice materials are tested with the objective of validating our simulation models. Finally, effects of all variables on compressive performance are examined and analyzed to generate guidelines for the design of metamaterial dual-phase composites for optimal mechanical performance.

2. Design and methods

2.1. Design

We designed our dual-phase lattices (DPLs) as mechanical metamaterial composites consisting of architected truss materials in the form of a matrix (MP) and reinforcement phase (RP), as illustrated in Fig. 1. The design space of metamaterials can be largely expanded by incorporating the second phase into architected materials with bioinspired phase patterning. However, the selection of the second phase and design interface represents the prevailing issue, as described below.

2.1.1. Variation in reinforcement phase architecture

To specifically examine how differing reinforcement phases and the nature of the phase boundary affects mechanical properties, dual-phase mechanical metamaterials were first contemplated with various RP topologies and geometries. As a baseline, face-centered cubic (*fcc*) lattice materials were selected for the matrix phase with a specific C-*fcc* form pattern for the RP where all the reinforcement grains were in contact (Fig. 1a). DPLs with nine types of RP architectures were then considered; these included a *bcc* type, *fcc* type, and *fcc* based hybrids which were composed of *fcc* and three elementary architecture including simple cubic (s), cross cubic (c) and edge center cubic (e). The forming DPLs were respectively named as *RP-bcc*, *RP-fcc*, *RP-fcc+c*, *RP-fcc+s*, *RP-fcc+e*, *RP-fcc+s+c*, *RP-fcc+c+e*, *RP-fcc+s+e*, *RP-fcc+s+c+e*, as shown in Fig. 1c.

Additionally, effects of the geometries of the RP were also examined in this study. Truss members in the *fcc* unit were divided into two categories: trusses within the cubic surface of diameter d_1, which were connected with surrounding lattice units, and those inside the cube of diameter d_2 that could be varied independently without affecting the architecture of the phase boundaries. Five types of DPLs, which were termed *RP-G1* to *RP-G5* depending upon their slenderness ratios (d_2/l), were also designed (Table S1) and examined.

2.1.2. Variation in connection phase architecture

Architectures in the connection phase (CP) in the immediate vicinity of the connection points between the reinforcement grains were also investigated; these in general determined the pattern of the reinforcement grains. The green blocks in Fig. 1 from the matrix phase were adjusted to form different connection phases. As such, five types of connection phase architectures were designed and examined to discern their effects on the mechanical performance of the DPLs. These architectures are termed as *CP-fcc*, *CP-fcc+s*, *CP-fcc+s+c*, *CP-fcc+s+c+e*, *CP-fcc+s+c+e+bcc*, as illustrated in Fig. 1d, with the *RP-fcc+s+c* type lattice fixed as the reinforcement phase.

2.1.3. Variation in architecture at phase boundaries

Dual-phase metamaterials with a maximum slip area at the phase boundaries, where every lattice unit in the matrix phase is completely surrounded by reinforcement phase lattice and designed with coherent phase boundaries, have been shown to exhibit optimal energy absorption capability [16]. Such behavior mimics the toughness of sea shells, such as the nacre layer in abalone shells, where small micrometer-scale displacements between the mineral "bricks" in their "brick-and-mortar" structure helps to dissipate the high stresses which would otherwise cause the mineral to fracture [9]. In the present study, we further examine the distinct role of the interface (Fig. 1e) on the mechanical properties of our DPLs by varying the architectural structure at the phase boundary. Eight types of phase-boundary architectures were designed, with the *RP-G3* type lattice fixed as the reinforcement phase. All geometrical parameters are summarized in Table S1.

2.2. Simulation and experimental methods

Finite element analysis (FEA) was performed as the primary strategy to investigate the effects of critical design parameters on the resulting mechanical properties, as designated above. An explicit dynamics finite element analysis approach was employed using LS-DYNA solutions (LS-DYNA, Livermore, USA). The dual-phase lattice models were built up using solid elements, with trusses of measured diameter and two stiff compression plates. To select the appropriate element size, a mesh convergence analysis was performed and an element size of 1.0 mm was employed to ensure accurate results with a high calculation efficiency. The material properties were set to be ideally elastoplastic in the simulation model [16]. In this model, two types of contacts were employed. An automatic general contact was adopted among lattice trusses, whereas node-to-surface contact was set up between the lattice trusses and compression plates.

However, to validate the above simulation model, experimental studies were also performed on metallic dual-phase mechanical metamaterials that were fabricated by additive manufacturing using stainless steel powders. Three types of DPLs were tested, including matrix phase single-phase lattices, *C-fcc* and Co-continuous *fcc* type DPLs termed *(Co-fcc).* These lattices were tested in compression on a universal electro-mechanical

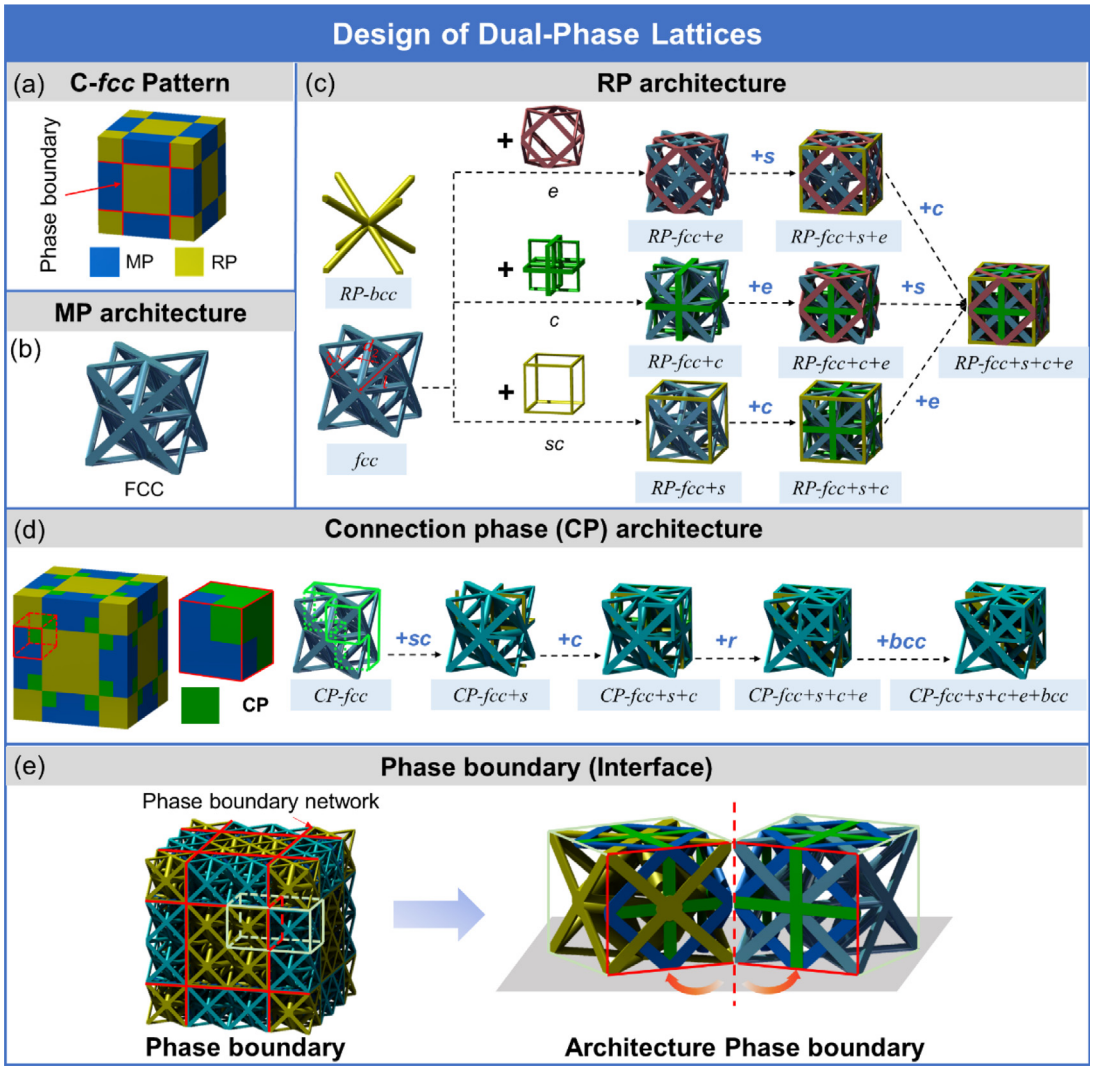

Fig. 1. Variation in architecture of the dual-phase lattices (DPLs). (a) A specific C-*fcc* form pattern of the reinforcement phase (RP) for all the DPLs. (b) Face-centered cubic (*fcc*) lattice materials were selected for the matrix phase (MP). (c) Nine types of RP architectures including *bcc* type, *fcc* type, and *fcc* based hybrids. (d) DPLs with an enhanced connection phase (CP) including five type of architectures. (e) Architectural enhancement at the phase boundary.. (For interpretation of the references to color in this figure legend, the reader is referred to the web version of this article.)

testing machine (MTS Exceed E64, MTS Systems China) at a constant cross-head strain rate of $\sim 10^{-3}$/s. Prior to testing, electron backscatter diffraction (EBSD) analysis was used to examine the crystal structure of the printed austenitic stainless-steel sections. Their meso-scale morphology was observed using a KEYENCE VHX-6000 optical microscope (Keyence, Osaka, Japan).

3. Results and discussion

3.1. Experimental results

The compressive engineering stress–strain curves and deformation modes are compared with the simulation results in Fig. 2a–b. Similar to our previous study [16], the matrix phase lattice materials failed by progressive crushing layer by layer while the *C-fcc* type DPLs (*RP-G3*) failed with localized shear bands that bypassed the interconnected reinforcement grains. Specifically, for the *Co-fcc* type DPLs with *fcc+s+c* type RP and CP architectures, the deformation was dominated by the interconnected reinforcement phase, such that the *fcc* type matrix phase was induced to deform in unison with the reinforcement phase, until densification of matrix phase occurred followed by that of the stronger RP. As shown in Fig. 2b, the simulated results generally agree well with experimentally measured stress–strain curves; the discrepancy apparent at large strains, especially in the Co-*fcc* type DPLs, can mainly be attributed to the non-uniformity of the trusses after printing (Fig. 2c), and the fact that nodal volume effects [20] could not be neglected. Note that the incorporation of boundary conditions caused only minimal effects on the mechanical properties; this is shown in Figure S3 where we have employed simulations of the stress–strain curves for the *C-fcc* and *Co-fcc* type DPLs with symmetric versus free boundary conditions. Inverse Pole Figure (IPF) maps in Fig. 2d show the microstructure and grain orientation of the stainless-steel segments of the trusses. The grain structure shows an average grain size of 5 μm with adjacent grains generally displaying orientation differences below 10°.

3.2. Reinforcement phase

3.2.1. Effects of reinforcement phase architecture

The compressive stress–strain curves and deformation modes for DPLs with various RP architectures were simulated and are compared in Fig. 3a and c. Generally, the compression characteristics of the dual-phase lattice materials with different RP

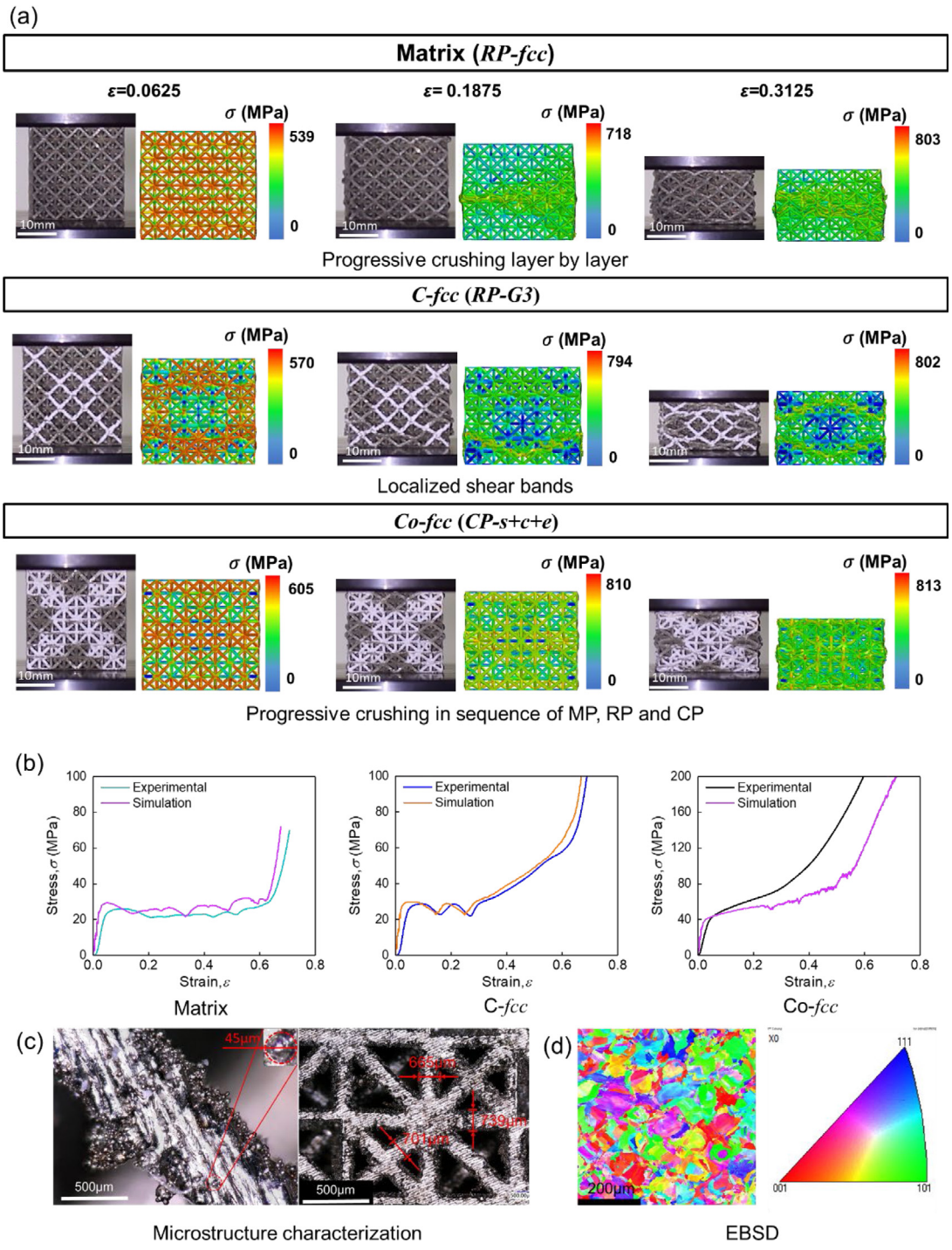

Fig. 2. Compression tests and morphology for three types of DPLs fabricated by selective laser melting. (a) Deformation modes and (b) stress–strain curves for three types of DPLs validated by simulation. (c) Mesoscopic truss morphology and (d) EBSD characterization.

architectures was quite similar. With the specific *fcc* type matrix phase lattice, when an *fcc* type lattice was also selected for the reinforcement phase which possessed the same strength, *i.e.*, the strength σ of the MP and RP are equal ($\sigma_{MP} = \sigma_{RP}$), the resulting single-phase lattice (SPL) materials displayed layer-by-layer truss buckling before finally failing by localized shear bands. As more elementary architectures were assembled in the RP, *i.e.*, where $\sigma_{MP} < \sigma_{RP}$, the stress to deform the lattices increased as a function of strain, especially above a strain of ~0.2 (Fig. 3c); this was concomitant with phase-boundary slip and localized shear bands bypassing the reinforcement grains. Akin to sea shells [9], such phase-boundary displacements serve to dissipate the effect of high local stresses; they represent a desired deformation mode in DPLs as the slip of reinforcement grains along the phase boundaries tends to accompany the twisting of the trusses, which additionally contributes to strain hardening and additional energy absorption. With the bending-dominated *bcc* type lattice employed as the reinforcement, where $\sigma_{MP} > \sigma_{RP}$, under compression the resulting DPLs first exhibited deformation in the reinforcement grains with plastic buckling of the trusses taking place around the phase boundaries; subsequently, X-shaped localized shear banding occurred which tended to bypass the stronger

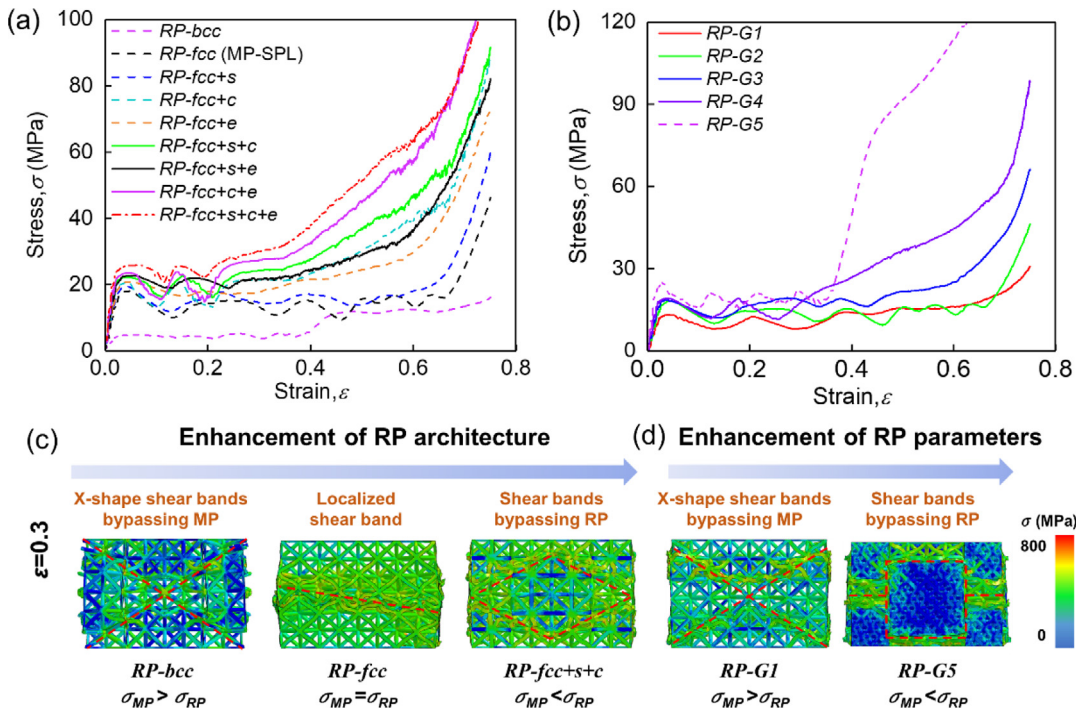

Fig. 3. Numerical simulation results for DPLs with various types of RP architectures and geometry. Compressive stress–strain curves for the DPLs with different (a) RP architectures and (b) geometries; typical deformation modes for the DPLs with different (c) RP architectures and (d) geometries.

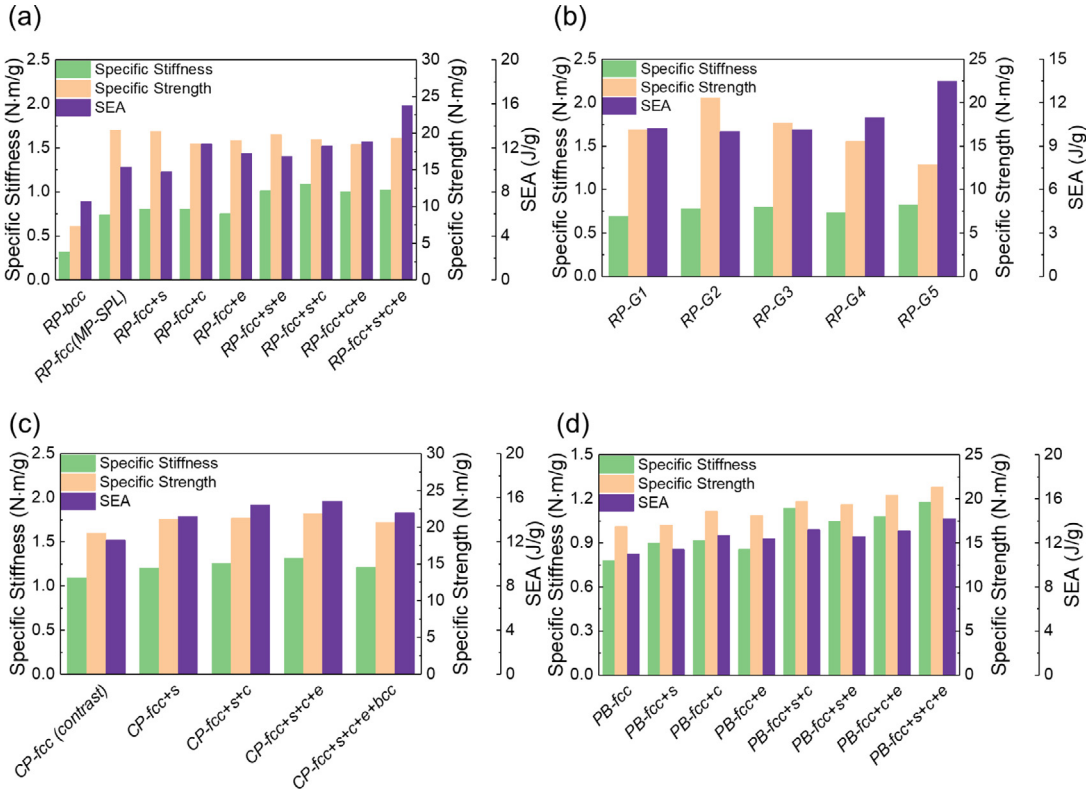

Fig. 4. Comparison of the simulations of the mechanical properties, namely specific stiffness, compressive strength, energy absorption per unit mass (SEA), of all types of the single-phase (SPLs) and dual-phase (DPLs) lattice structures. (a–d) DPLs with various (a) RP architectures, (b) RP geometries, (c) CP architectures, (d) phase-boundary architectures.

matrix phase lattice. More information about these deformation modes in DPLs with various RP architectures is shown in Figure S1.

The simulated specific stiffness, specific strength and energy absorption per unit mass (specific energy absorption, SEA) of all the SPLs and DPLs are compared and summarized in Fig. 4:

- The specific stiffness of the DPLs varied with architecture; specifically those with *RP-fcc+s+c* type reinforcements displayed superior specific stiffness to those with the more complex *RP-fcc+s+c+e* type reinforcements. Elementary architectures *s* and *c* in particular exhibited outstanding specific stiffness, as shown by simulation results in Figure S2, because their trusses were distributed along the compression direction. Designing more trusses into the RP architecture along the loading direction clearly represents an effective way to increase the specific stiffness of DPLs.
- With respect to strength, from our previous study [16] the strength of the DPLs was primarily controlled by that of the MP and the nature of its connections with the reinforcement phase; accordingly, the nature of the RP architecture had little effect on strength properties (Fig. 4a).
- The energy absorption properties of the lattice structures, conversely, were enhanced when the difference in the densification stress of the MP and RP was made as large as possible [16]. Accordingly, the specific energy absorption (SEA) increased as more elementary architectures were incorporated into the DPLs. This can be readily seen in Fig. 4a where the SEA of the *RP-fcc+s+c+e* type DPLs was 55% larger than that of *fcc* type single phase lattice.

3.2.2. Effects of reinforcement phase geometry

In addition to architecture, the relative density of the RP can also affect the mechanical properties of DPLs. Using numerical simulations, this was considered with *fcc* type RPs, where the slenderness ratio of trusses inside the lattice cubic (with diameter d_2 and length l (Fig. 1c)) was varied. The simulation results revealed that the structures needed a higher stress to sustain a specific level of strain with the increase of relative density when the dimensions d_2 increased or l decreased. When the slenderness ratio of the inside trusses was decreased to d_2/l ~0.09 (RP-G1), the strength of the matrix phase exceeded that of the reinforcement phase ($\sigma_{MP} > \sigma_{RP}$), such that the reinforcement grains deformed first with X-shaped localized shear bands subsequently bypassing the matrix phase lattice. In contrast, when the slenderness ratio of the trusses increased to d_2/l ~0.28 (RP-G5), the RP hardly deformed at all ($\sigma_{MP} < \sigma_{RP}$) even if the MP was completely deformed; in this case, compressive failure occurred via rectangular-shape shear bands (Fig. 3d). However, as shown in Fig. 4b, the specific stiffness and energy absorption of the DPLs increased slightly with increasing diameter d_2, which can be attributed to the fact that the trusses were no longer effectively arranged along the compressive loading direction. At the same time, the specific strength decreased in comparison to that of the *fcc* type single phase lattice (RP-G2), because the strength of the DPLs was primarily controlled by the connections between the reinforcement grains. Similarly, as the truss length l was reduced from 4.24 mm to 2.12 mm (RP-G5 in Table S1), the specific stiffness and energy absorption were both enhanced with the SEA for this architecture being the highest; indeed, it was as much as 11% larger than that of the *fcc* type single phase lattice (RP-G2).

3.3. Connection phase

The connections among the reinforcement grains have been shown to have a marked effect on the strength of DPLs [16]. Here, numerical simulations were performed for DPLs with five types of architectures for the connection phase; results are presented in Fig. 4c, 5a and c. These structures needed a higher stress to sustain a specific level of strain as more elementary architectures were incorporated into the CP. When the stiffness and strength of the CP (*fcc+s+c* type) was increased to match that of the RP, torsional distortion occurred at the connection point nodes that link the reinforcement grains, which in turn induced more severe deformation resulting in an additional contribution to the energy absorption. Essentially, as the CP was made stiffer and stronger than the RP, both the MP and RP deformed simultaneously followed by the CP until failure.

The incorporation of elementary architectures into the CP significantly increased the specific stiffness, strength and energy absorption of the DPLs, as shown in Fig. 4c. The *CP-fcc+s+c+e* type DPLs displayed the best combination of properties, with specific stiffness, strength, and energy absorption values, respectively, 77%, 7% and 51% larger than the *fcc* type MP. Also, with these complex architectures, the specific stiffness and energy absorption of the Co-*fcc* DPL (CP-*fcc+s*) can be markedly higher than the reinforcement phase, namely respectively ~50% and 15% higher than that of RP-*fcc+s*. Accordingly, we can conclude that it is important to incorporate trusses that are oriented along the loading direction in order to generate DPLs with significantly improved mechanical properties compared to the original C-*fcc* type DPLs.

3.4. Phase boundary

As noted above, maximizing the phase-boundary slip area can definitively enhance the energy absorption capability of the lattice structures. In light of this, the architectures of the interface structures at the phase boundary were examined, and DPLs with various truss topologies at the phase boundary were correspondingly simulated and compared; this is shown in Fig. 4 and 5b. For the specific C-*fcc* type DPLs, the reinforcement grains were arranged to be in contact with an interface network created among the phase boundaries; this was further consolidated by systematically incorporating more elementary architectures at the interface, as illustrated in Fig. 1e. Numerical simulations were then employed to model the modes of deformation and resulting mechanical properties of these DPLs under compressive loading. The simulation results showed that torsional deformation occurred at the connection points linking the reinforcement grains, accompanied by marked deformation and further plastic buckling of the trusses near the phase boundaries, as shown in Fig. 5d. Also, a higher stress was needed to sustain a specific level of strain with these reinforced interface architectures, as shown in Fig. 5b. The specific stiffness and SEA values of these DPLs with reinforced phase boundaries were, respectively, 59% and 39% larger than those of the *fcc* type MP SPLs; however, although stronger, the specific strength of the DPLs was rarely increased due to the increase in relative density associated with the additional weight of the reinforced phase boundaries.

4. Conclusions

Strong and tough dual-phase mechanical metamaterials have been designed through bioinspired lattice phase patterning. In this study, we examined a selection of mesoscale architectures for each lattice phase and their interfaces using both simulation and experiment to guide the design of dual-phase lattices (DPLs) with enhanced energy absorption capability under uniaxial compression loading. Based on our experimental results and simulations, the following conclusions can be made:

(1) Enlarging the difference in strength between the matrix (MP) and reinforcement (RP) phases serves to increase the plastic deformation of the trusses at the phase boundaries. By ensuring that more trusses in the reinforcement phase (RP) are distributed along the loading direction, this markedly improves the specific stiffness and energy absorption of the lattice structure.

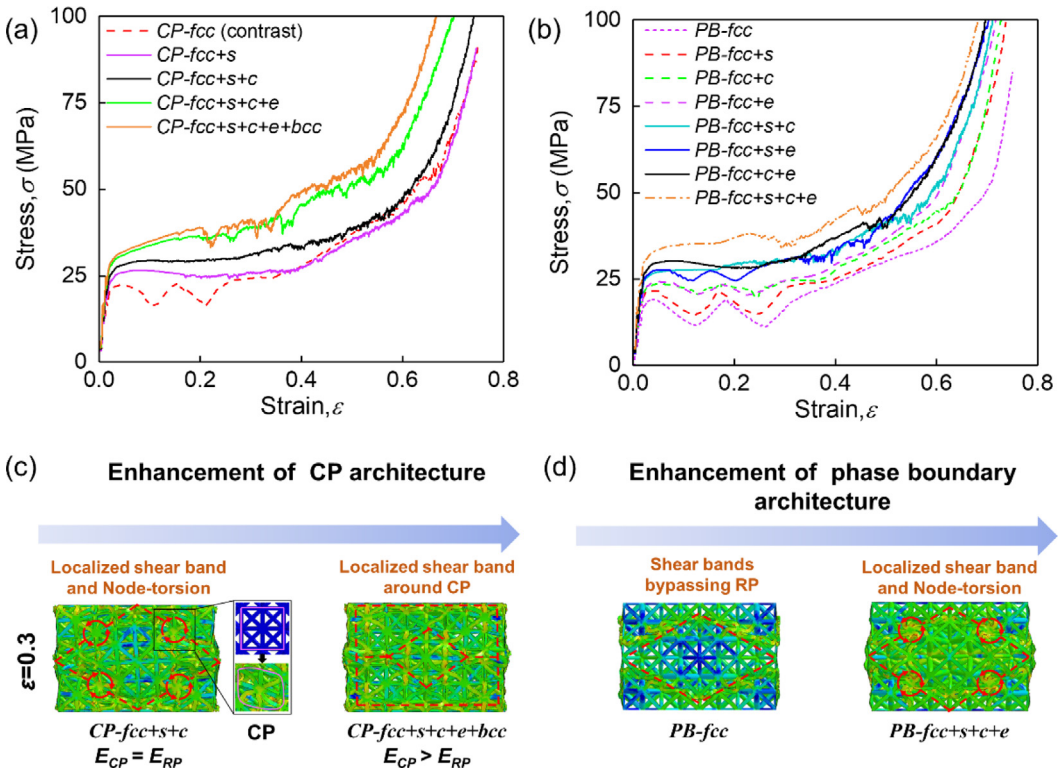

Fig. 5. Numerical simulation results for DPLs with various types of CP architectures and phase-boundary architectures. Compressive stress–strain curves for the DPLs with different (a) CP architectures, (b) phase-boundary geometries; typical deformation modes for three types of DPLs with different (c) CP architectures, (d) phase-boundary geometries.

(2) When the connection phase (CP) is both stiffer and stronger than the RP, the sequence of deformation of the DPLs occurs primarily in the MP, followed by the RP and ultimately the CP before failure. With reinforced connections, torsional distortion of the nodes is observed instead of phase-boundary slip. Such enhanced CPs can optimize the mechanical properties of the DPLs, including specific stiffness and strength, and specific energy absorption.
(3) The interface network can be enhanced by the variation in truss topologies, which can slightly increase the specific stiffness and specific energy absorption of the DPLs.

In summary, based on the above analysis, in addition to the guidelines given in our previous study, we can conclude that stiffness is mainly determined by the orientation of the trusses, with trusses distributed along the loading direction being the most efficient. Strength, conversely, is primarily controlled by the connections between the reinforcement grains. Additionally, the toughness or specific energy absorption is determined by the phase-boundary area [16], the densification of stress and strain, and the strength difference between the two phases. Accordingly, cautious architecture selection of the constituent phases, *i.e.*, the reinforcement phase, connection phase and phase boundaries, together with bioinspired phase patterning, can further increase the energy absorption capability and expand the design space of dual-phase lattice metamaterials. However, these guidelines are still not complete as the optimal bounds may also be affected by the deformation mode and Poisson's ratio effect of each phase, which still requires further investigation.

CRediT authorship contribution statement

Weihua Guo: Methodology, Software, Visualization, Writing – original draft. **Yao Huang:** Formal analysis, Visualization. **Robert O. Ritchie:** Supervision, Writing – review & editing. **Sha Yin:** Conceptualization, Supervision, Methodology, Writing – review & editing.

Declaration of competing interest

The authors declare that they have no known competing financial interests or personal relationships that could have appeared to influence the work reported in this paper.

Acknowledgments

This work was supported by the Fundamental Research Funds for the Central Universities, China, Beihang University, and BUAA-CAIP Lightweight Research Institute supported by Jiangsu Changshu Automotive Trim Group Co., Ltd, China. ROR acknowledges support from the H.T. & Jessie Chua Distinguished Professorship, USA at Berkeley.

Appendix A. Supplementary data

Supplementary material related to this article can be found online at https://doi.org/10.1016/j.eml.2021.101442.

References

[1] S.D. Lucas R. Meza, J.R. Greer, Strong, lightweight, and recoverable three-dimensional ceramic nanolattices, Science 345 (2020) 1322–1326, http://dx.doi.org/10.1126/science.1255908.
[2] D. Mohr, Elastically-isotropic truss lattice materials of reduced plastic anisotropy, Int. J. Solids Struct. 138 (2018) 24–39, http://dx.doi.org/10.1016/j.ijsolstr.2017.12.025.
[3] R. Gümrük, R.A.W. Mines, Compressive behaviour of stainless steel micro-lattice structures, Int. J. Mech. Sci. 68 (2013) 125–139, http://dx.doi.org/10.1016/j.ijmecsci.2013.01.006.

[4] S.C. Han, J.W. Lee, K. Kang, A new type of low density material: Shellular, Adv. Mater. 27 (2015) 5506–5511, http://dx.doi.org/10.1002/adma.201501546.
[5] X. Chen, Q. Ji, J. Wei, H. Tan, J. Yu, P. Zhang, V. Laude, M. Kadic, Lightweight shell-lattice metamaterials for mechanical shock absorption, Int. J. Mech. Sci. 169 (2020) http://dx.doi.org/10.1016/j.ijmecsci.2019.105288.
[6] C. Bonatti, D. Mohr, Large deformation response of additively-manufactured FCC metamaterials: From octet truss lattices towards continuous shell mesostructures, Int. J. Plast. 92 (2017) 122–147, http://dx.doi.org/10.1016/j.ijplas.2017.02.003.
[7] H.S. Lei, C.L. Li, X.Y. Zhang, P.D. Wang, H. Zhou, Z.A. Zhao, D.N. Fang, Deformation behavior of heterogeneous multi-morphology lattice core hybrid structures, Additive Manuf. 37 (2021) http://dx.doi.org/10.1016/j.addma.2020.101674.
[8] H. Yang, L. Ma, 1D to 3D multi-stable architected materials with zero Poisson's ratio and controllable thermal expansion, Mater. Des. 188 (2020) http://dx.doi.org/10.1016/j.matdes.2019.108430.
[9] U.G.K. Wegst, H. Bai, E. Saiz, A.P. Tomsia, R.O. Ritchie, Bioinspired structural materials, Nature Mater. 14 (2015) 23–36, http://dx.doi.org/10.1038/nmat.4089.
[10] A. Velasco-Hogan, J. Xu, M.A. Meyers, Additive manufacturing as a method to design and optimize bioinspired structures, Adv. Mater. 30 (2018) 1800940, http://dx.doi.org/10.1002/adma.201800940.
[11] S. Yin, H. Chen, J. Li, T.X. Yu, J. Xu, Effects of architecture level on mechanical properties of hierarchical lattice materials, Int. J. Mech. Sci. 157–158 (2019) 282–292, http://dx.doi.org/10.1016/j.ijmecsci.2019.04.051.
[12] E. Munch, M.E. Launey, D.H. Alsem, E. Saiz, A.P. Tomsia, R.O. Ritchie, Tough, bio-inspired hybrid materials, Science 322 (2008) 1516–1520, http://dx.doi.org/10.1126/science.1164865.
[13] L. Wang, J. Lau, E.L. Thomas, M.C. Boyce, Co-continuous composite materials for stiffness, strength, and energy dissipation, Adv. Mater. 23 (2011) 1524–1529, http://dx.doi.org/10.1002/adma.201003956.
[14] J.H. Lee, L. Wang, M.C. Boyce, E.L. Thomas, Periodic bicontinuous composites for high specific energy absorption, Nano Lett. 12 (2012) 4392–4396, http://dx.doi.org/10.1021/nl302234f.
[15] Y. Liu, L. Wang, Enhanced. stiffness, Enhanced stiffness strength and energy absorption for co-continuous composites with liquid filler, Compos. Struct. 128 (2015) 274–283, http://dx.doi.org/10.1016/j.compstruct.2015.03.064.
[16] S. Yin, W. Guo, H. Wang, Y. Huang, R. Yang, Z. Hu, D. Chen, J. Xu, R.O. Ritchie, Strong and tough bioinspired additive-manufactured dual-phase mechanical metamaterial composites, J. Mech. Phys. Solids 149 (2021) 104341, http://dx.doi.org/10.1016/j.jmps.2021.104341.
[17] T. Kamae, L.T. Drzal, Carbon fiber/epoxy composite property enhancement through incorporation of carbon nanotubes at the fiber–matrix interphase – Part I: The development of carbon nanotube coated carbon fibers and the evaluation of their adhesion, Compos. Part A 43 (2012) 1569–1577, http://dx.doi.org/10.1016/j.compositesa.2012.02.016.
[18] Z. Hu, Y. Fu, Z. Hong, Y. Huang, W. Guo, R. Yang, J. Xu, L. Zhou, S. Yin, Composite structural batteries with Co_3O_4/CNT modified carbon fibers as anode: Computational insights on the interfacial behavior, Compos. Sci. Technol. 201 (2021) http://dx.doi.org/10.1016/j.compscitech.2020.108495.
[19] B. Liu, X. Feng, S.M. Zhang, The effiective Young's modulus of composites beyond the voigt estimation due to the Poisson effect, Compos. Sci. Technol. 69 (2009) http://dx.doi.org/10.1016/j.compscitech.2009.06.004.
[20] H. Yan, X. Yang, T. Lu, G. Xie, Mechanical properties of copper octet-truss nanolattices, J. Mech. Phys. Solids 101 (2017) 133–149, http://dx.doi.org/10.1016/j.jmps.2017.01.019.